

Temporally Robust Multi-Agent STL Motion Planning in Continuous Time

Joris Verhagen¹, Lars Lindemann² and Jana Tumova¹

Abstract—Signal Temporal Logic (STL) is a formal language over continuous-time signals (such as trajectories of a multi-agent system) that allows for the specification of complex spatial and temporal system requirements (such as staying sufficiently close to each other within certain time intervals). To promote robustness in multi-agent motion planning with such complex requirements, we consider motion planning with the goal of maximizing the temporal robustness of their joint STL specification, i.e. maximizing the permissible time shifts of each agent’s trajectory while still satisfying the STL specification. Previous methods presented temporally robust motion planning and control in a discrete-time Mixed Integer Linear Programming (MILP) optimization scheme. In contrast, we parameterize the trajectory by continuous Bézier curves, where the curvature and the time-traversal of the trajectory are parameterized individually. We show an algorithm generating continuous-time temporally robust trajectories and prove soundness of our approach. Moreover, we empirically show that our parametrization realizes this with a considerable speed-up compared to state-of-the-art methods based on constant interval time discretization.

I. INTRODUCTION

Robustness of motion plans is often associated with the extent to which a signal can be spatially perturbed while still guaranteeing safety or desired performance. An example of this is specifying a robot to stay away from a wall where a door might suddenly open. Robustness is then increased by increasing the distance to the wall, promoting safety in such unforeseen events. We can however imagine scenarios where robustness is needed against temporal perturbations. This becomes especially apparent in multi-robot systems where robots need to collaborate or avoid each other, and where individual delays may result in task violation. Consider for example a robot-to-robot handover task where two robots should stay close enough for the handover to happen. During the execution of a pre-planned motion strategy, unmodeled dynamics, environmental factors, localization issues, and even onboard timing issues may cause one robot to be delayed, after which the other robot has already departed to fulfill the next part of its specification. An example of this is shown in Fig. 1. In these scenarios, it is clear that the

This work was partially supported by the Wallenberg AI, Autonomous Systems and Software Program (WASP) funded by the Knut and Alice Wallenberg Foundation.

¹Joris Verhagen and Jana Tumova are with the Division of Robotics, Perception and Learning, School of Electrical Engineering and Computer Science, KTH Royal Institute of Technology, Stockholm, Sweden
{jorisv, tumova} @kth.se

²Lars Lindemann is with the Thomas Lord Department of Computer Science, University of Southern California, Los Angeles CA, USA
llindema@usc.edu

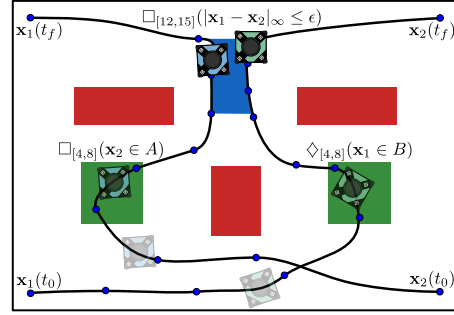


Fig. 1. An example of a multi-agent STL specification. Two robots are required to be close enough to each other for a predetermined amount of time (blue) in addition to an individual spatio-temporal requirement (green). To ensure the time robustness of the collaborative task, we need to consider time shifts on both trajectories.

temporal robustness of motion plans is of vital importance as it allows agents to arrive earlier or later than planned while still meeting a specification. Specifically towards multi-robot systems, we are interested in the maximization of Asynchronous Temporal Robustness (ATR) [1], which considers the time shifts of individual agents within a predicate, i.e. agents being delayed or arriving early. We subsequently wish to generate feasible motion plans for multi-agent systems that maximize the ATR of a spatio-temporal specification.

A. Contributions

In this work, we consider double-integrator, continuous-time multi-agent systems subjected to a fragment of bounded time STL with linear predicates. We develop upon existing works that consider discrete-time temporal robustness via the constant-interval discretization of a system’s trajectory. However, in contrast to state of the art, we optimize the continuous-time temporal robustness. The contributions of our work are summarized as follows:

- We present an efficient multi-agent Bézier curve parametrization of the system’s trajectory that allows for reasoning over continuous space and time. We empirically demonstrate that this continuous time may lead to the theoretically optimal temporal robustness of a motion plan.
- We propose a Mixed-Integer Linear Program (MILP) that finds a continuous multi-agent motion plan that is robust to asynchronous time shifts, and we show its soundness.
- We provide a theoretical analysis of computational complexity and empirical evidence of speed-up compared to methods based on time discretization.

B. Related Work

To formulate tasks in both spatial and temporal domains, temporal logics such as Linear Temporal Logic (LTL) have been employed. Although LTL allows temporal ordering, it does not allow the user to reason over time quantitatively. Addressing these limitations are methods such as Metric Temporal Logic and Signal Temporal Logic (STL) [2]. As STL allows reasoning over continuous-time signals, we are interested in maximizing the temporal robustness of specifications that consider a fragment of this temporal logic.

As STL can account for continuous signals, it allows for direct reasoning over the robustness of spatio-temporal missions. Many existing works consider spatial robustness of STL specifications in motion planning [3]–[5] based on the definition of robust semantics in [6] and [7]. In time-critical systems, however, it is not enough to consider spatial robustness. In collaborative multi-robot systems, for example, we wish to consider maximizing temporal robustness, which has been given less attention. Work in [8] defines temporal robustness on predicate shifts on a small fragment of STL. Full (time-bounded) STL with predicate shifts is considered in [9], [10]. Although it does not consider individual shifts of signals within a predicate, the work in [11] combines left- and right-temporal robustness (accommodating advancements and delays respectively) to generate motion plans that are robust to time shifts in both directions. Asynchronous Temporal Robustness (ATR), formally defined in [1], is used as a constraint in [12]. In a similar vein, the authors in [13], [14] present counting LTL (cLTL) which is able to bound asynchronous shifts in discrete space and time. Related is also the work in [15] which concerns temporal relaxations. In contrast, we aim to not just constrain the ATR, but to directly maximize it. Further, all these works rely on a constant-time discretization of the trajectory, fundamentally limiting the resolution of both the trajectory and its temporal robustness while also requiring a high number of variables for long-horizon missions. To this end, we represent trajectories with independent space- and time parametrization.

Multi-agent STL motion planning with independent space and time parametrization was introduced in [16] where piecewise linear segments are concatenated to satisfy qualitative semantics of STL specifications. The trajectory formulation in this work generalizes this by using a Bézier parametrization from [17] in a multi-agent context that allows for non-constant velocity segments, continuous differentiability, and, as we will show, quantitative temporal semantics of STL.

II. PRELIMINARIES

Let \mathbb{R} and \mathbb{N} be the set of real and natural numbers including zero, respectively, and let $\mathbb{R}_{\geq 0}$ denote the set of real, non-negative numbers. Let $\mathbb{B} = \{\top, \perp\}$, where \top and \perp indicate the Boolean true and false values. Additionally, let $\mathbf{x}(t) \in \mathbb{R}^{\dim \cdot n}$ be the state of a multi-agent system at time $t \in \mathbb{R}_{\geq 0}$ where $\mathbf{x}_k(t) \in \mathbb{R}^{\dim}, k \in \{1, \dots, n\}$ is regarded as the state of agent k , and n is the number of agents. The mapping $\mathbf{x} : \mathbb{R}_{\geq 0} \rightarrow \mathbb{R}^{\dim \cdot n}$ is a *signal*. Lastly, let $\mathbb{R}^{p \times q}$ be a p by q matrix of real numbers.

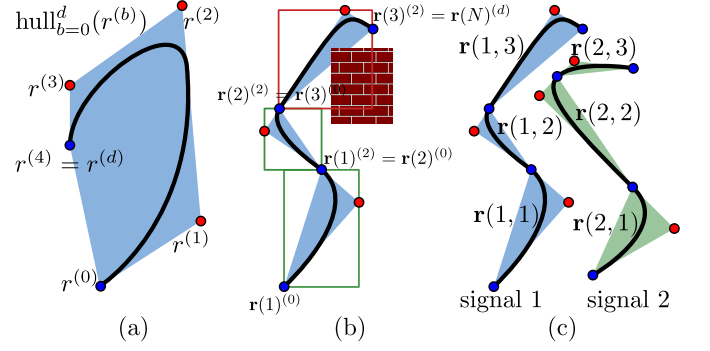


Fig. 2. (a) A Bézier curve with its control points and its convex hull (in light blue). $r^{(b)}$ indicates the b 'th control point of r . (b) A concatenation of 3 Bézier curves with their convex hulls. Consideration of the bounding box for obstacle avoidance. $r_{(2)}^{(2)}$ is not collision-free according to the conservativeness of Eq. (28). (c) Multi-agent Bézier parametrization indicating segments of r_k for $k = 1$ and $k = 2$.

A. Bézier curves

Our approach relies on Bézier curves that have found many use cases in motion planning of autonomous systems [17], [18]. A Bézier curve is represented by a polynomial equation and parameterized by a finite number of control points, its decision variables. Namely, a Bézier curve r of degree d is constructed and evaluated using the summation of its d Bernstein polynomials multiplied with their respective d control points according to

$$r(s) := \sum_{b=0}^d \binom{d}{b} (1-s)^{d-b} s^b \cdot r^{(b)}, \quad s \in [0, 1], \quad (1)$$

where s is the phasing parameter, $\binom{d}{b} (1-s)^{d-b} s^b$ is the b 'th Bernstein polynomial, and $r^{(b)}$ is the b 'th control point. An example of a Bézier curve with its control points is shown in Fig. 2a. Although Bézier curves are nonlinear in nature, the following properties allow us to reason over their convex over-approximation:

- 1) *Convex hull*: the curve $r(s)$ is entirely contained within the convex hull generated by its control points $r^{(b)}$, $r(s) \in \text{hull}_{b=0}^d(r^{(b)}) \quad \forall s \in [0, 1]$, shown in Fig. 2a.
- 2) *Endpoint values*: the curve $r(s)$ starts at the first control point $r^{(0)}$ as $s = 0$ and ends at the last control point $r^{(d)}$ as $s = 1$.
- 3) *Derivatives*: the derivative $\dot{r}(s) = \frac{dr(s)}{ds}$ is a linear combination of the control points of $r(s)$ and is again a Bézier curve of degree $d - 1$ with control points $\dot{r}^{(b)} = d \cdot (r^{(b+1)} - r^{(b)})$ for $b = \{0, \dots, d - 1\}$.

Subsequently, the derivatives of the start- and end-point, $\dot{r}^{(0)}$ and $\dot{r}^{(d-1)}$, are linear combinations of the control points of $r(s)$ and the convex hull of \dot{r} is formed as a linear combination of its control points. This means that smooth, kinematically feasible, and collision-free trajectories can be constructed through Linear Programming by returning a finite set of control points of a Bézier curve.

B. Signal Temporal Logic

Signal Temporal Logic (STL) [2] considers real-valued signals making it a powerful tool for specifying and verifying properties of dynamical systems. Let us first define a fragment of STL that we use in this work that specifies desired properties of n -dimensional, finite, continuous-time signals $\mathbf{x} : \mathbb{R}_{\geq 0} \rightarrow X \subseteq \mathbb{R}^n$.

Definition 1 (Fragment of Signal Temporal Logic). *Let bounded time intervals I be in the form $[t_1, t_2]$, where, for all, $I \subset \mathbb{R}_{\geq 0}$, $t_1, t_2 \in \mathbb{R}_{\geq 0}$, $t_1 \leq t_2$. Let $\mu : X \rightarrow \mathbb{R}$ be a linear real-valued function, and let $p : X \rightarrow \mathbb{B}$ be a linear predicate defined according to the relation $p(\mathbf{x}) := \mu(\mathbf{x}) \geq 0$. The set of predicates is denoted AP . We consider a fragment of STL, recursively defined as*

$$\begin{aligned}\psi &:= p \mid \diamond_I p \mid \square_I p \\ \phi &:= \psi \mid \psi_1 \wedge \psi_2 \mid \psi_1 \vee \psi_2\end{aligned}\quad (2)$$

where $p \in AP$. The symbols \wedge and \vee denote the Boolean operators for conjunction and disjunction, respectively; and \diamond_I and \square_I denote the temporal operator Eventually and Always.

In the STL fragment, we consider the bounded *Always* and *Eventually* operators, (requiring to have a predicate hold for all time $t \in I$ and for any time $t \in I$, respectively) and allow conjunctions and disjunctions of any combinations of these.

C. Time-Robust Semantics of STL

The qualitative semantics of STL indicate whether a signal \mathbf{x} satisfies a specification ϕ or not. However, we wish to additionally specify how robustly a signal satisfies the specification. To that end, we use a version of Asynchronous Temporal Robustness (ATR) semantics inspired by [1]. We call the variant *recursive ATR*; it defines the allowed time shifts on the states of the agents in a multi-agent system for a predicate p , and further recursively for the fragment of STL introduced in Def. 1. Intuitively, the ATR indicates to what extent the state \mathbf{x}_k of each agent k can be shifted in time asynchronously with respect to the states of other agents, while still having the entire system's state \mathbf{x} satisfying the specification ϕ . This property becomes especially interesting in multi-agent systems, where agents are subject to individual time-shifts, but a joint specification. For example, for the system in Fig. 1, such a joint specification is "Always, between 12 and 15 seconds, robot 1 and robot 2 should be ϵ -close".

First, let $\mathcal{S}_p = \{k_1, \dots, k_m\}$ be the set of indices of all agents that influence the truth value of predicate p . Let the relevant state vector for predicate p be defined as $\mathbf{x}_p(t) = [\mathbf{x}_{k_1}(t), \dots, \mathbf{x}_{k_m}(t)]^T, \forall k_i \in \mathcal{S}_p$. With respect to the example in Fig. 1, $\mathcal{S}_p = \{1, 2\}$ and $\mathbf{x}_p(t) = [\mathbf{x}_1(t), \mathbf{x}_2(t)]^T$.

Definition 2 (Recursive ATR). *Let us define the time-shifted state that is relevant to predicate p as $\mathbf{x}_{p,\bar{\kappa}}(t)$, with time shift $\bar{\kappa} := \{\kappa_k \mid k \in \mathcal{S}_p\} \in \mathbb{R}^m$, $m = |\mathcal{S}_p|$ as*

$$\mathbf{x}_{p,\bar{\kappa}}(t) := [\mathbf{x}_{k_1}(t + \kappa_{k_1}), \dots, \mathbf{x}_{k_m}(t + \kappa_{k_m})]^T \quad \forall k \in \mathcal{S}_p. \quad (3)$$

where $\mathbf{x}_{p,\bar{\kappa}}(t) \in \mathbb{R}^{dim \cdot m}$. Regardless of the dimensionality of the workspace, an agent is subjected to a single, unique, time shift; $\bar{\kappa} \in \mathbb{R}^m$ while $\mathbf{x}_{p,\bar{\kappa}}(t) \in \mathbb{R}^{dim \cdot m}$.

The recursive ATR first defines the maximum extent the state of each agent $l \in \mathcal{S}_p$ may be shifted in time asynchronously such that the predicate still holds.

$$\bar{\theta}_p(\mathbf{x}, t) := \bar{\chi}_p(\mathbf{x}_p, t).$$

$$\max \left\{ \tau \geq 0 : \begin{array}{l} \kappa_l \in [-\tau, \tau], \forall l \in \mathcal{S}_p, \\ \bar{\chi}_p(\mathbf{x}_{p,\bar{\kappa}}, t) = \bar{\chi}_p(\mathbf{x}_p, t) \end{array} \right\}, \quad (4)$$

where $\bar{\chi}^p$ is the characteristic function, defined as

$$\bar{\chi}_p(\mathbf{x}, t) := \begin{cases} 1, & \text{if } \mu(\mathbf{x}, t) \geq 0 \\ -1, & \text{else} \end{cases} \quad (5)$$

We additionally define ATR recursively for the temporal and Boolean operators of the STL fragment in Eq. (2).

$$\begin{aligned}\bar{\theta}_{\square_I p}(\mathbf{x}) &:= \min_{t' \in I} (\bar{\theta}_p(\mathbf{x}, t')), \\ \bar{\theta}_{\diamond_I p}(\mathbf{x}) &:= \max_{t' \in I} (\bar{\theta}_p(\mathbf{x}, t')), \\ \bar{\theta}_{\phi_1 \wedge \phi_2}(\mathbf{x}) &:= \min(\bar{\theta}_{\phi_1}(\mathbf{x}), \bar{\theta}_{\phi_2}(\mathbf{x})), \\ \bar{\theta}_{\phi_1 \vee \phi_2}(\mathbf{x}) &:= \max(\bar{\theta}_{\phi_1}(\mathbf{x}), \bar{\theta}_{\phi_2}(\mathbf{x})).\end{aligned}\quad (6)$$

obtaining the ATR of specification ϕ as $\bar{\theta}_\phi$.

A non-negative ATR indicates the extent to which the state of all agents may be time-shifted asynchronously while still satisfying the predicate p . In contrast, negative ATR indicates the minimum extent to which the state of each agent needs to be shifted in time to change from violation of p to its satisfaction.

Remark 1. *When a predicate is dependent on a single agent, e.g. $\square_{[4,8]}(\mathbf{x}_2 \in A)$ as per Fig. 1, the Recursive ATR collapses to the combined left- and right temporal robustness of [11], defining temporal robustness via the maximum permissible shift of the temporal interval I .*

Lemma 1. *For the ATR $\bar{\theta}_\phi$, it follows that $\max(|\kappa_{k_1}|, \dots, |\kappa_{k_m}|) \leq |\bar{\theta}_\phi| \implies \bar{\chi}_\phi(\mathbf{x}_{\bar{\kappa}}) = \bar{\chi}_\phi(\mathbf{x})$.*

Proof Sketch. Notice that Def. 2 states that $\bar{\theta}_p(\mathbf{x}, t) = c$ indicates that $\forall \kappa_{k_1}, \dots, \kappa_{k_m} \in [-c, c]$ we have that the shifted signal $\mathbf{x}_{p,\bar{\kappa}}(t)$ also satisfying predicate p . $\bar{\theta}_{\square_I p}(\mathbf{x}) = c$ subsequently states that $\forall t \in I, \bar{\theta}_p(\mathbf{x}, t) \geq \bar{\theta}_{\square_I p}(\mathbf{x}) = c$ ensuring ATR for all times $t \in I$ of at least c . Conversely, $\bar{\theta}_{\diamond_I p}(\mathbf{x}) = c$ states that $\exists t \in I, \bar{\theta}_p(\mathbf{x}, t) = \bar{\theta}_{\square_I p}(\mathbf{x}) = c$ ensuring ATR for a time $t \in I$ of c . The Boolean operators are trivial. Given the fragment in Eq. (2) this concludes the proof sketch. \square

III. PROBLEM STATEMENT

Consider a double-integrator, continuous-time multi-agent dynamical system of the form

$$\ddot{\mathbf{x}}(t) = \mathbf{u}(t), \quad \mathbf{x}(t_0) = \mathbf{x}_{t_0}, \dot{\mathbf{x}}(t_0) = \dot{\mathbf{x}}_{t_0}, \quad (7)$$

where $\mathbf{x} \in \mathbb{R}^{dim \cdot n}$ is a stacked vector of the states $\mathbf{x}_k \in \mathbb{R}^{dim}$ of the agents, with dim being the dimension of the workspace and n the number of agents. The system is subject to an

initial- and final state \mathbf{x}_{t_0} and \mathbf{x}_{t_f} at initial- and final time t_0 and t_f , velocity constraints $\dot{\mathbf{x}} \in \mathcal{V} = [\underline{\dot{\mathbf{x}}}, \bar{\dot{\mathbf{x}}}]$ for all agents, and a spatial-temporal mission ϕ expressed from the fragment of STL in Eq. (2). Additionally, consider the workspace \mathcal{W} as a convex polygon with convex polygon obstacles \mathcal{W}_{obs} , defining the free workspace as $\mathcal{W}_{free} = \mathcal{W} \setminus \mathcal{W}_{obs}$. We aim to find a collision-free motion plan that maximizes the ATR $\bar{\theta}_\phi^*$ from Def. 2. As such, we wish to obtain a continuous-time control input such that the corresponding trajectory $\mathbf{x}^*(t)$ satisfies the specification ϕ with the ATR $\bar{\theta}_\phi^*$. Subsequently, we define the optimization problem

$$\underset{\mathbf{u}}{\operatorname{argmax}} \quad \bar{\theta}_\phi(\mathbf{x}) \quad (8)$$

$$\text{s.t. } \ddot{\mathbf{x}}(t) = \mathbf{u}(t), \forall t \in [t_0, t_f], \quad (8a)$$

$$\bar{\theta}_\phi(\mathbf{x}) > 0, \quad (8b)$$

$$\mathbf{x}(t_0) = \mathbf{x}_{t_0}, \mathbf{x}(t_f) = \mathbf{x}_{t_f}, \quad (8c)$$

$$\mathbf{x}_k(t) \in \mathcal{W}_{free}, \forall t \in [t_0, t_f], \forall k \in \{1, \dots, n\}, \quad (8d)$$

$$\dot{\mathbf{x}}_k(t) \in \mathcal{V}, \forall t \in [t_0, t_f], \forall k \in \{1, \dots, n\}. \quad (8e)$$

In contrast to existing problem definitions, we consider a continuous-time system and maximizing the continuous-time asynchronous temporal robustness which has not been, to the best of our knowledge, performed before.

IV. MULTI-AGENT BÉZIER PARAMETRIZATION

As we are concerned with specifications that are expressed both in the spatial and temporal domains, we wish to use a trajectory formulation that allows us to reason over these dimensions separately. To that end, we define a *curvature Bézier curve* $r(s)$ and a *temporal Bézier curve* $t := h(s)$. We then couple these curves to parameterize the physical trajectory over time. We base our multi-agent Bézier formulation on the work in [17] where the authors express a trajectory segment x via the use of $r(s)$ and $h(s)$ as follows:

$$r(s) := x(h(s)), \quad (9)$$

$$\dot{r}(s) := \dot{x}(h(s))\dot{h}(s). \quad (10)$$

It should be noted that x is our physical trajectory of interest, which is parameterized by the two types of Bézier curves.

A. Trajectory Construction

Consider a space of dimension $\dim \cdot n$ (e.g., n agents modeled as the double integrator from Eq. (7) moving in a 2D environment). To generate the full trajectory of a single agent k , we concatenate N Bézier curve (*segments*), denoted as $\mathbf{r}(k) \in \mathcal{B}^{\dim \times N}$ and $\mathbf{h}(k) \in \mathcal{B}^N$, where \mathcal{B} indicates the set of Bézier curves. An example of the concatenation of curvature Bézier curves is shown in Fig. 2b.

For a multi-agent system consisting of n agents, we consider n concatenations of the aforementioned, leading to the system parametrization by \mathbf{r} and \mathbf{h} . Given agents $k \in \{1, \dots, n\}$ and segments $i \in \{1, \dots, N\}$, the function \mathbf{r} is defined as $\mathbf{r} : \{1, \dots, n\} \times \{1, \dots, N\} \rightarrow \mathcal{B}^{\dim}$ returning a vector of curvature Bézier curves. The function \mathbf{h} is defined as $\mathbf{h} : \{1, \dots, n\} \times \{1, \dots, N\} \rightarrow \mathcal{B}$ returning a temporal

Bézier curve. The b 'th control point of the temporal Bézier curve of agent k at segment i is denoted by $\mathbf{h}(k, i)^{(b)}$ and similarly for the curvature, $\mathbf{r}(k, i)^{(b)}$, as shown in Fig. 2.

B. Continuity Constraints

To realize the double integrator dynamics of Eq. (7), we ensure continuous differentiability of x between. We do this in a conservative yet linear manner for each agent $k \in \{1, \dots, n\}$ by constraining the first and last (i.e. d -th for a Bézier curve of degree d) control points of each segment i according to

$$\begin{aligned} \mathbf{r}(k, i)^{(d)} &= \mathbf{r}(k, i+1)^{(0)} \wedge \mathbf{h}(k, i)^{(d)} = \mathbf{h}(k, i+1)^{(0)} \\ \Rightarrow \mathbf{x}_k(i) &= \mathbf{x}_k(i+1) \end{aligned} \quad (11)$$

$$\begin{aligned} \dot{\mathbf{r}}(k, i)^{(d-1)} &= \dot{\mathbf{r}}(k, i+1)^{(0)} \wedge \dot{\mathbf{h}}(k, i)^{(d-1)} = \dot{\mathbf{h}}(k, i+1)^{(0)} \\ \Rightarrow \dot{\mathbf{x}}_k(i) &= \dot{\mathbf{x}}_k(i+1). \end{aligned} \quad (12)$$

We constrain the initial and final time, t_0 and t_f , and the forward traversal of time via

$$\mathbf{h}(k, 0)^{(0)} = t_0, \quad (13)$$

$$\mathbf{h}(k, N)^{(d)} = t_f, \quad (14)$$

$$\dot{\mathbf{h}}(k, i)^{(b)} > 0 \quad \forall i \in \{1, \dots, N\}, \forall b \in \{0, \dots, d-1\}, \quad (15)$$

for each agent $k \in \{1, \dots, n\}$. The Bézier formulation allows us to consider the maximization problem $\operatorname{argmax}_{\mathbf{r}, \mathbf{h}}$ as opposed to $\operatorname{argmax}_{\mathbf{u}}$ in Eq. (8) as the acceleration, $\ddot{\mathbf{x}}$, is implicitly parameterized by the curvature and time Béziers \mathbf{r} and \mathbf{h} due to the derivative properties of Bézier curves as per Sec. II-A.

V. RECURSIVE ATR ON BÉZIER SEGMENTS

The definition of recursive ATR in Def. 2 cannot directly be implemented in a motion planning framework, as it is defined over strictly continuous time signals. Instead, we would like to be able to evaluate temporal robustness at a finite set of points. As such, we consider a definition of recursive ATR that considers non-constant time segments from the Bézier parametrization in Sec. IV. In the following, in accordance with the constraint in Eq. (8b), we restrict ourselves to strictly positive definitions of temporal robustness. We will show that under this assumption, the recursive ATR on non-singular time segments is sound and an underapproximation of $\bar{\theta}_\phi(\mathbf{x})$.

Let $I_{(k, i)} = [\mathbf{h}(k, i)^{(0)}, \mathbf{h}(k, i)^{(d)}]$ be the time-span of segment i of agent k , see Fig. 3 and assume it is not a single point. Segment Recursive ATR considers allowed segment shifts on the states of individual agents.

Definition 3 (Segment Recursive ATR). *Consider the time-shifted state $\mathbf{x}_{p, \bar{R}}(t)$ from Eq. (3). First, for a predicate p , Segment Recursive ATR for an agent $k \in \mathcal{S}_p$ and a segment $i \in \{1, \dots, N\}$ defines the maximum extent the state of each agent $l \in \mathcal{S}_p$, including k , may shift asynchronously such that all segments spanning the original time-span of segment i ,*

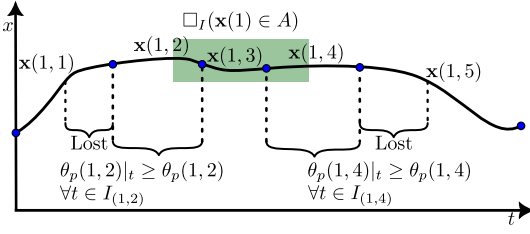


Fig. 3. Example of Always staying within a certain range $x \in A$ for a certain time interval I . Notice the under-approximation of the true temporal robustness of Def. 2 as the $\theta_p(k, i)$ is assigned the lower-bound of $\theta_p(k, i)|_t, \forall t \in I_{(k, i)}$ and the end-point evaluation of the Bézier curve (Lost).

$I_{(k, i)}$, satisfy $\chi_p(k, i)$.

$$\theta_p(\mathbf{x}, k, i) := \chi_p(\mathbf{x}_p, k, i).$$

$$\max \left\{ \tau \geq 0 : \begin{array}{l} \bar{\kappa} \in [-\tau, \tau], \forall l \in \mathcal{S}_p, \\ \chi_p(\mathbf{x}_{p, \bar{\kappa}}, k, j) = \chi_p(\mathbf{x}_p, k, i), \forall j \in J(\tau) \end{array} \right\}, \quad (16)$$

where $\chi_p(\mathbf{x}_p, k, i)$ is the characteristic function for a segment i of agent k ,

$$\chi_p(\mathbf{x}_p, k, i) := \begin{cases} 1, & \text{if } \mu(\mathbf{x}_p, t) \geq 0 \quad \forall t \in I_{(k, i)} \\ -1, & \text{otherwise,} \end{cases} \quad (17)$$

which relies on evaluating the predicate for all control points of segment i . The set $J(\tau)$ is dependent on τ and defined as

$$J(\tau) := \{j \in \{1, \dots, N\} \mid \exists \kappa_k \in [-\tau, \tau] : I_{(k, j)} + \kappa_k \cap I_{(k, i)} \neq \emptyset\}. \quad (18)$$

We additionally define Segment Recursive ATR for the temporal operators of the STL fragment in Eq. (2) as

$$\theta_{\square_{IP}}(\mathbf{x}, k) := \min_{i \in \{1, \dots, N\}, I_{(k, i)} \cap I \neq \emptyset} (\theta_p(\mathbf{x}, k, i)), \quad (19)$$

$$\theta_{\square_{IP}}(\mathbf{x}) := \min_{k \in \mathcal{S}_p} (\theta_{\square_{IP}}(\mathbf{x}, k)), \quad (20)$$

$$\theta_{\diamond_{IP}}(\mathbf{x}, k) := \max_{i \in \{1, \dots, N\}, I_{(k, i)} \cap I \neq \emptyset} (\theta_p(\mathbf{x}, k, i)), \quad (21)$$

$$\theta_{\diamond_{IP}}(\mathbf{x}) := \min_{k \in \mathcal{S}_p} (\theta_{\diamond_{IP}}(\mathbf{x}, k)), \quad (22)$$

and for the Boolean operators as

$$\theta_{\phi_1 \wedge \phi_2}(\mathbf{x}) := \min(\theta_{\phi_1}(\mathbf{x}), \theta_{\phi_2}(\mathbf{x})), \quad (23)$$

$$\theta_{\phi_1 \vee \phi_2}(\mathbf{x}) := \max(\theta_{\phi_1}(\mathbf{x}), \theta_{\phi_2}(\mathbf{x})),$$

obtaining the ATR of specification ϕ as $\theta_{\phi}(\mathbf{x})$.

The set J indicates all segments of k that now intersect or have intersected the original time span of segment i under the time-shift $\kappa_k \in [-\tau, \tau]$, which includes i itself.

Theorem 1. For positive ATR, $\theta_{\phi}(\mathbf{x}) \leq \bar{\theta}_{\phi}(\mathbf{x})$, indicating an underapproximation of the ATR from Def. 2.

Proof. First, we show that $\theta_p(\mathbf{x}, k, i) \leq \bar{\theta}_p(\mathbf{x}, t)$, for all $t \in I_{(k, i)}$. From Eq. (17) it follows that $\chi_p(\mathbf{x}, k, i) \leq \bar{\chi}_p(\mathbf{x}, t)$, for all $t \in I_{(k, i)}$. Note that we assume that $\chi_p(\mathbf{x}, k, i) = 1$. From Eq. (17) and Eq. (18), it follows that for all $\bar{\kappa}$, if $\chi_p(\mathbf{x}_{p, \bar{\kappa}}, k, j) = \chi_p(\mathbf{x}, k, i) = 1, \forall j \in J(\tau)$,

then also $\bar{\chi}_p(\mathbf{x}_{p, \bar{\kappa}}, t) = \bar{\chi}_p(\mathbf{x}, t) = 1, \forall t \in I_{(k, i)}$. Hence, $\chi_p(\mathbf{x}_{p, \bar{\kappa}}, k, j) \leq \bar{\chi}_p(\mathbf{x}_{p, \bar{\kappa}}, t), \forall j \in J, t \in I_{(k, i)}$. Hence, $\tau^* \leq \bar{\tau}^*$, where τ^* is the maximizing τ in Eq. 16 and similarly $\bar{\tau}^*$ is the maximizing $\bar{\tau}$ in Eq. 4. Considering the positive value of the characteristic function, altogether we have $\theta_p(\mathbf{x}, k, i) \leq \bar{\theta}_p(\mathbf{x}, t)$.

Next, consider $\theta_{\square_{IP}}(\mathbf{x}, k)$. As we have established that $\theta_p(\mathbf{x}, k, i) \leq \bar{\theta}_p(\mathbf{x}, t), \forall t \in I_{(k, i)}$, we can state that $\theta_p(\mathbf{x}, k, i) \leq \bar{\theta}_p(\mathbf{x}, t), \forall t \in (I \cap I_{(k, i)})$. Hence, consider that by taking min over all segments i for which $I_{(k, i)} \cap I \neq \emptyset$ we obtain a temporal robustness $\theta_{\square_{IP}}(\mathbf{x}, k) \leq \bar{\theta}_{\square_{IP}}(\mathbf{x}, t)$. To obtain the overall ATR, θ_{\square_I} , we need to consider each agent $k \in \mathcal{S}_p$ as described in Eq. (20). From Def. 3 it follows that $\bar{\theta}_{\square_{IP}}(\mathbf{x}, k) = \bar{\theta}_{\square_{IP}}(\mathbf{x}, l), \forall k, l \in \mathcal{S}_p$ and hence by taking the min over all agents we obtain $\theta_{\square_{IP}}(\mathbf{x}) \leq \bar{\theta}_{\square_{IP}}(\mathbf{x})$.

Next, consider $\theta_{\diamond_{IP}}(\mathbf{x}, k)$. Consider that by taking max over all segments i for which $I_{(k, i)} \cap I \neq \emptyset$ we obtain a temporal robustness $\theta_{\diamond_{IP}}(\mathbf{x}, k) \leq \bar{\theta}_{\diamond_{IP}}(\mathbf{x})$. Similar to \square_{IP} , we consider each agent in \mathcal{S}_p and obtain $\theta_{\diamond_{IP}}(\mathbf{x}) \leq \bar{\theta}_{\diamond_{IP}}(\mathbf{x})$.

The binary \wedge and \vee are trivial. Given the considered fragment of Eq. (2), this concludes the proof. \square

Remark 2. As $N \rightarrow \infty$, Segment Recursive ATR collapses to Recursive ATR in Def. 2 as $\theta_{\square_{IP}}(\mathbf{x}, k) = \theta_{\square_{IP}}(\mathbf{x}, l), \forall k, l \in \mathcal{S}_p$ and $\theta_p(\mathbf{x}, k, i) \rightarrow \bar{\theta}_p(\mathbf{x}, t)$ as $I_{(k, i)} \rightarrow t$.

We redefine the problem in Sec. III by maximizing the segment recursive ATR, $\theta_{\phi}(\mathbf{x})$, as opposed to $\bar{\theta}_{\phi}(\mathbf{x})$ in Eq. (8) and constraining satisfaction by $\theta_{\phi}(\mathbf{x}) > 0$ as opposed to $\bar{\theta}_{\phi}(\mathbf{x}) > 0$ in Eq. (8b).

VI. MILP ENCODING

In this section, we will address the computation of Bézier parametrization that can handle general motion planning constraints, STL specifications, and their temporal robustness. We will specifically elaborate on how Segment Recursive ATR from Def. 3 is implemented in a MILP.

A. Trajectory Constraints

Let us first define the trajectory constraints from Eq. (8a), (8c), (8d), and (8e) with the Bézier parametrization from Sec. IV. First, we constrain the initial and final state of the trajectory (corresponding to Eq. (8c)) by constraining the first and last control point of the position and velocity of the first and last segment respectively, according to

$$\mathbf{x}_k(t_0) = \mathbf{x}_{k, t_0} \iff \mathbf{r}(k, 0)^{(0)} = \mathbf{x}_{k, t_0} \quad (24)$$

$$\dot{\mathbf{x}}_k(t_0) = \dot{\mathbf{x}}_{k, t_0} \iff \dot{\mathbf{r}}(k, 0)^{(0)} = \dot{\mathbf{h}}(k, 0)^{(0)} \dot{\mathbf{x}}_{k, t_0}, \quad (25)$$

$$\mathbf{x}_k(t_f) = \mathbf{x}_{k, t_f} \iff \mathbf{r}(k, N)^{(d)} = \mathbf{x}_{k, t_f}, \quad (26)$$

$$\dot{\mathbf{x}}_k(t_f) = \dot{\mathbf{x}}_{k, t_f} \iff \dot{\mathbf{r}}(k, N)^{(d-1)} = \dot{\mathbf{h}}(k, N)^{(d-1)} \dot{\mathbf{x}}_{k, t_f}. \quad (27)$$

We then address constraint Eq. (8d) by introducing a constraint that each control point of segment i of agent k lies within the convex polygon workspace and that all control points of segment i of agent k lay outside at least one face

of every convex obstacle polygon

$$\mathbf{x}_k(i) \in \mathcal{W}_{\text{free}} \iff \bigwedge_{f=1}^{n_w^{\text{faces}}} \bigwedge_{j=0}^d (b_w^f - H_w^f \mathbf{r}(k, i)^{(j)} \geq 0) \wedge \bigwedge_{l=1}^{n_{\text{obs}}} \bigvee_{f=1}^{n_l^{\text{faces}}} \bigwedge_{j=0}^d (b_l^f - H_l^f \mathbf{r}(k, i)^{(j)} \leq 0), \quad (28)$$

where n_{obs} defines the number of obstacles, n_w^{faces} defines the number of faces of the world polygon, $\mathcal{W}_{\text{free}}$, and n_l^{faces} defines the number of faces of obstacle polygon l , H_w^f and b_w^f are the f 'th row of the matrix and vector for the half-space inequality conditions of the convex *world* polygon. $H_l^k f$ and b_l^f denote the equivalent for obstacle l . An example of this is shown in Fig. 2b.

Lastly, we constrain the velocity (constraint in Eq. (8e))

$$\dot{\mathbf{x}}_k(i) \in \mathcal{V} \iff \dot{\mathbf{h}}(k, i)^{(j)} \underline{\dot{\mathbf{x}}}_k \leq \dot{\mathbf{r}}(k, i)^{(j)} \leq \dot{\mathbf{h}}(k, i)^{(j)} \bar{\dot{\mathbf{x}}}_k, \quad \forall j \in \{0, \dots, d-1\}. \quad (29)$$

Notice the workspace and velocity constraints, (28) and (29), rely on the convex-hull overapproximation and bounding box and can be conservative.

B. STL Constraints

We use $\theta_p^{\pm \dots \pm}(\mathbf{x}, k, i)$, where $\pm \in \{+, -\}$, to denote the temporal robustness of predicate p for agent k at segment i where multiple agents influence the truth value of the predicate. For example, if $S_p = \{k, l\}$, $\theta_p^{+-}(\mathbf{x}, k, i)$ indicates that signal k is shifted to the right and signal $l, l \neq k$ is shifted to the left. It hence captures the shifts $\forall \kappa_k \in [0, \tau], \kappa_l \in [-\tau, 0]$. Similarly $\theta_p^{++}(\mathbf{x}, k, i)$ captures the shifts $\forall \kappa_k, \kappa_l \in [0, \tau]$, etc. $\theta_p^{\pm \dots \pm}(\mathbf{x}, k, i)$ is then the overall robustness of p , regardless of the direction of the time shift, equivalent to Eq. (16). We also use $\theta_p^{0 \pm \dots \pm}(\mathbf{x}, k, i)$, where $\pm \in \{+, -\}$ to indicate the temporal robustness when agent k is not subject to a time shift, while the other agents $l \in S_p, l \neq k$ are.

1) *Predicates*: Let us first define the satisfaction of a predicate for a Bézier segment i of agent k . A Bézier curve can only be evaluated in a linear fashion at the first and last control point. In order to keep computations feasible, we define satisfaction of a predicate p for the segment i via the bounding box of segment i . For stay-in polygon predicate p , this would result in the indicator variable $z_{(k,i)}^{\text{spat}} \in \mathbb{B}$ for satisfaction of predicate p for the segment i of agent k according to

$$z_{(k,i)}^{\text{spat}} = \bigwedge_{f=1}^{n_{\text{faces}}} \bigwedge_{j=0}^d (b^f - H^f \mathbf{r}(k, i)^{(j)} \geq 0). \quad (30)$$

We can additionally consider interdependent predicates, for example, $\mu = (|\mathbf{x}_1 - \mathbf{x}_2|_\infty \leq \epsilon)$ from Fig. 1. Given that each agent has its own temporal curve per segment, $\mathbf{h}(k, i) : \{1, \dots, n\} \times \{1, \dots, N\} \rightarrow \mathcal{B}$, we can only look at predicate

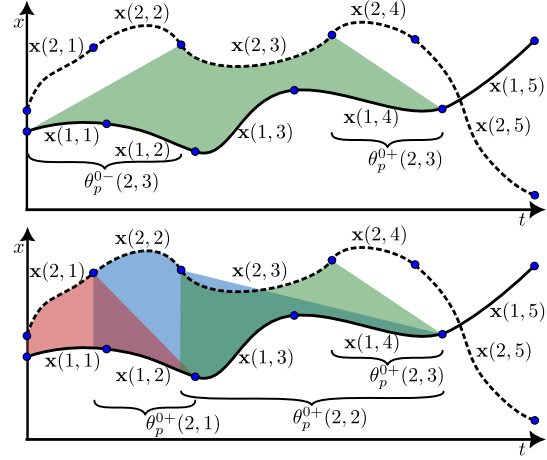


Fig. 4. Top: Right and left temporal robustness of the third index of agent 2 with respect to shifts in the state of agent 1 for predicate $p = \mathbf{x}_1 \leq \mathbf{x}_2$. Bottom: Right temporal robustness of indices of agent 2 w.r.t. agent 1, where the state of agent 2 is static. we need to consider these when we look at the ATR of segment 3 of agent 2.

satisfaction by first considering the intersections of Bézier segments between agents via

$$z_{(k,i),(l,j)}^{\text{temp}} := \{I_{(k,i)} \cap I_{(l,j)} \neq \emptyset\}, \quad (31)$$

where $z_{(k,i),(l,j)}^{\text{temp}} \in \mathbb{B}$ is a variable indicating whether segment i of agent k and segment j of agent l intersect. We can obtain the equivalent of Eq. (30) for predicates that depend on the states of multiple agents

$$z_{(k,i)}^{\text{spat}} := \bigwedge_{j \in J(\tau)} z_{(k,i),(l,j)}^{\text{temp}} \quad \forall j : z_{(k,i),(l,j)}^{\text{temp}} = \top, \forall l \in S_p, l \neq k, \quad (32)$$

that states that $z_{(k,i)}^{\text{spat}} \in \mathbb{B}$ is true if and only if all segments of agent l that intersect segment i of agent k satisfy the predicate function. For a predicate p that is dependent on 3 agents, this would result in a tensor of indicator variables $z^{\text{spat}} \in \mathbb{B}^{N \times N \times N}$.

Implementing the segment recursive ATR from Def. 3 for agent k and segment i relies on several steps:

- 1) First, for each agent $l \in S_p, l \neq k$, we create two indicator arrays. $z_{(l,\cdot)(k,i)}^+ \in \mathbb{B}^N$ indicates the segments of l that appear after intersecting $I_{(k,i)}$, $z_{(l,\cdot)(k,i)}^- \in \mathbb{B}^N$ indicates the segments of agent l that appear before intersecting

$$z_{(l,\cdot)(k,i)}^+ = \{j \mid \mathbf{h}(l, j)^{(d)} \geq \mathbf{h}(k, i)^{(d)}\}, \quad (33)$$

$$z_{(l,\cdot)(k,i)}^- = \{j \mid \mathbf{h}(l, j)^{(0)} \leq \mathbf{h}(k, i)^{(0)}\}. \quad (34)$$

For the example illustrated in Fig. 4,

$$z_{(1,\cdot),(2,2)}^+ = [0 \ 0 \ 0 \ 1 \ 1]$$

$$z_{(1,\cdot),(2,2)}^- = [1 \ 1 \ 0 \ 0 \ 0]$$

with respect to segment $I_{(k,i)} = I_{(2,2)}$.

- 2) As we need to consider the temporal robustness of the segments $j \in J(\tau)$ per Eq. (3), we first obtain the temporal robustness for segment i of agent k while the

state of agent k is static for all combinatorial time shifts of agent $l \in \mathcal{S}_p, l \neq k$, e.g., $\theta_p^{0+ \dots}(k, i), \theta_p^{0+ \dots}(k, i), \theta_p^{0- \dots}(k, i), \theta_p^{0- \dots}(k, i)$, etc. We obtain $\theta_p^{0\pm \dots}(k, i)$ by considering the minimum duration $\forall l \in \mathcal{S}_p$ when $\chi_{(l,j)}^p \neq \chi_{(k,i)}^p$ occurs for the first time and $z_{(l,),(k,i)}^+ = 1$ or $z_{(l,),(k,i)}^- = 1$ depending on the direction of the shift under consideration. For obtaining $\theta_p^{0+}(k, i)$, we consider an $N \times 1$ column of $z^{spat} \in \mathbb{B}^{N \times N}$.

For the example in Fig. 4, agent 2 and segment 2, we obtain

$$z_{(2,2)}^{spat} = [1 \ 1 \ 1 \ 1 \ 0]$$

for which $\theta_p^{0+}(2, 2) = \mathbf{h}(1, 4)^{(0)} - \mathbf{h}(2, 2)^{(d)}$, i.e. the first occurrence of $\chi_p(l, j) \neq \chi_p(k, i)$. Equivalently, $\theta_p^{0-}(2, 2) = \mathbf{h}(2, 2)^{(0)} - \mathbf{h}(1, 0)^{(0)}$.

3) Then, realize that according to Def. 3, the state of agent k shifts and as such, element i gets replaced by $j \in J$ in accordance to Eq. (18). As such, for all combinatorial shifts in $\theta_p^{0\pm \dots}(k, i)$, for $\pm \in \{+, -\}$, we consider the forward and backward (or right and left) shift of the state of agent k . This results in $\theta_p^{+\pm \dots}(k, i)$ and $\theta_p^{-\pm \dots}(k, i)$. We construct $\theta_p^{+\pm \dots}(k, i)$ by adding the segment durations $I_{(k,j)}, j \in J(\tau), j \leq i$ to $\theta_p^{+\pm \dots}(k, i)$ only if there is sufficient temporal robustness of $\theta_p^{+\pm \dots}(k, j)$ for the predicate to hold when $I_{(k,j)} \cap I_{(k,i)} \neq \emptyset$.

An example of this is indicated in Fig. 4 in the bottom for a predicate dependent on the state of two agents.

4) At last, we obtain the Segment Recursive ATR of segment i of agent k as

$$\theta_p(\mathbf{x}, k, i) := \min(\theta_p^{+\pm \dots}(\mathbf{x}, k, i), \theta_p^{-\pm \dots}(\mathbf{x}, k, i)). \quad (35)$$

The above procedure is followed for each agent $l \in \mathcal{S}_p$ for each segment $i \in \{1, \dots, N\}$. We cannot translate the recursive ATR $\theta_p(k, i)$ to any of the segments of agent $l, l \neq k$ due to the non-constant duration of the Bézier segments.

2) *Temporal and Binary Operators:* The temporal and binary operators are directly applied via Eq. (20) - (23). It should be noted that these definitions mean that while our temporal robustness is continuous, it is evaluated at a discrete number of points in space. We obtain $\theta_\phi(\mathbf{x})$ and solve Eq. (8) with the underapproximation of $\theta_\phi(\mathbf{x}) \leq \bar{\theta}_\phi(\mathbf{x})$ for the cost and the constraint (8b).

C. Computational Complexity

For a multi-agent predicate, p , we approximate its complexity in the optimization problem by considering the binary variables needed to express its ATR. The complexity is

$$\mathcal{O}(N^{|\mathcal{S}_p|}) \quad (36)$$

where N is the number of segments and $|\mathcal{S}_p|$ indicates the number of agents affecting the truth value of predicate p .

Though the complexity is exponential, the Bézier formulation with non-constant segment durations allows for a

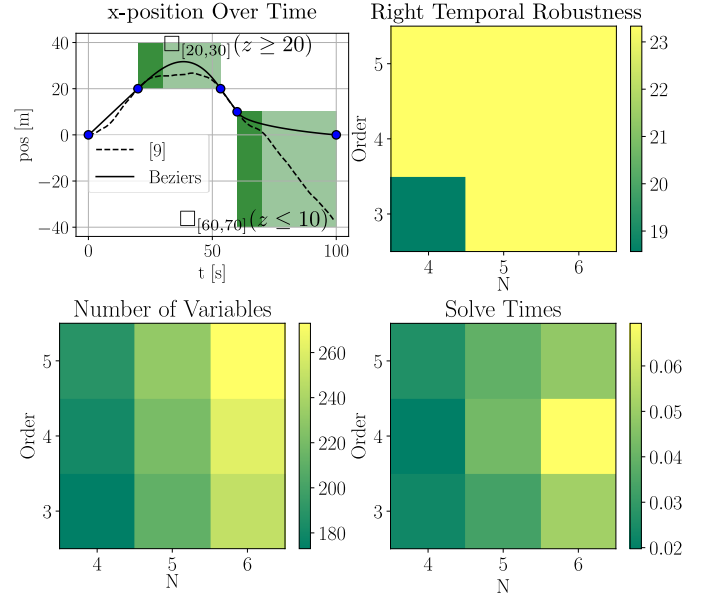


Fig. 5. Single-agent STL specification ϕ_{uav} for $N = d = 4$. Darker green indicates the predicate (and its duration), and lighter shades indicates the temporal robustness. Heatmaps indicate the dependency on the order and the number of Bézier curves in finding the optimal solution.

relatively low number of segments N , regardless of long-horizon missions, as the duration of a single temporal curve could be large. This will become apparent in the next section.

VII. RESULTS

We will show how our Bézier MILP implementation of temporal robust motion planning is computationally faster compared to constant discretization MILP implementations in [9] while obtaining a continuous-time underapproximation of the theoretically optimal temporal robustness. Additionally, we show how we are able to directly optimize the ATR of a specification. We will compare our method to a scenario in [9] to highlight the theoretical maximum temporal robustness and conclude by highlighting the optimization capabilities of our approach. Note that compared to [9], we are unable to handle acceleration constraints and do not allow nesting of temporal operators. However, we are able to compute continuous-time plans. We implement the left- and/or right-temporal robustness via the counting procedure described in [9], but consider the non-constant Bézier segment duration.

All simulations are performed on an Intel Core 12700H processor with 32 Gb of RAM. The method is implemented in Python and solved with Gurobi 10.0 [19].

A. Single-agent Case

Consider the altitude control of a one-dimensional UAV moving along the z -axis with state $\mathbf{x} = [z, \dot{z}]^T \in \mathbb{R}^2$, initial state $\mathbf{x}_0 = [0, 0]^T$, linear second-order dynamics, velocity bounds $|\dot{z}|_\infty \leq 1.5$, and the specification $\phi_{uav} = \square_{[20,30]}(z \geq 20) \wedge \square_{[60,70]}(z \leq 10)$. We remove the control input constraints from the benchmark. The simulation results are shown in Fig. 5.

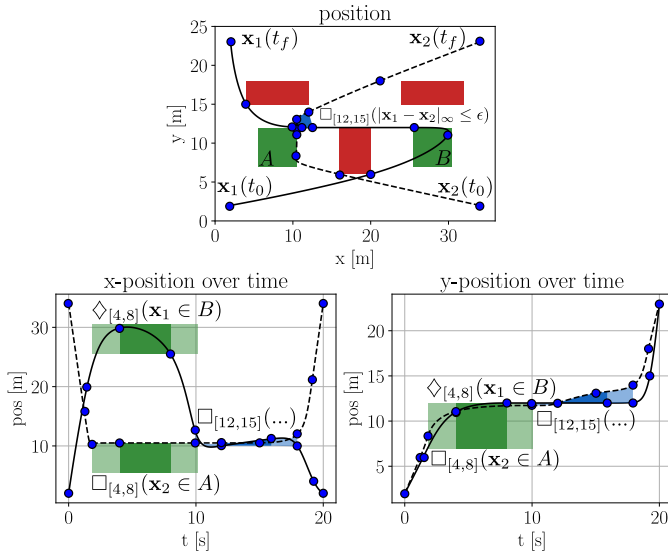


Fig. 6. ATR multi-agent example from Eq. (37). Darker shades indicate the predicate (and predicate duration), and lighter shades indicate the ATR of that predicate. Blue indicates $\square_{[12,15]}(|x_1 - x_2|_\infty \leq 1)$. The result allows any combinatorial shift of signal x_1 and x_2 up to $|\kappa_i| = \theta_{\phi_{MA}}(\mathbf{x}) = 2.03$.

The MILP formulation in [9] requires 100 1-second segments and obtains a maximum right temporal robustness of 23 seconds, limited by the discretization of 1-second intervals. Meanwhile, our Bézier formulation with only 4 segments obtains the theoretically maximal right temporal robustness of 23.33 seconds. Over 10 trials, [9] takes an average of 0.646 seconds while our Bézier method takes 0.019 seconds to compute.

B. Multi-agent Scenario

To assess the capabilities of maximizing the ATR of a multi-agent specification, we present the scenario from Fig. 1 and maximize its ATR. We describe the agents as double integrators subjected to the specification

$$\begin{aligned} \phi_{MA} = \diamondsuit_{[4,8]}(x_1 \in B) \wedge \square_{[4,8]}(x_2 \in A) \wedge \\ \square_{[12,15]}(|x_1 - x_2|_\infty \leq 1), \quad (37) \end{aligned}$$

where \mathbf{x}_1 and $\mathbf{x}_2 \in \mathbb{R}^2$ represent the position of robots 1 and 2 respectively. We consider the robots to be points for the sake of simplicity. We obtain the ATR $\theta_{\phi_{MA}}(\mathbf{x}) = 2.03$ seconds after 43 seconds of computation. The results are shown in Fig. 6. Notice that compared to the illustrative example in Fig. 1, the *Eventually* specification for agent 1, $\diamondsuit_{[4,8]}(x_1 \in B)$, motivates meeting near A in order to maximize the ATR. The formulation will find the optimal meeting place in terms of temporal robustness.

VIII. CONCLUSIONS

We have presented a continuous-time motion planner that considers the maximization of the asynchronous temporal robustness of an STL specification. Our Bézier trajectory parametrization was shown to significantly speed up the robustness maximization of single-agent predicates. We have

shown the soundness of our approach to generating asynchronous temporally robust trajectories and have shown its efficacy in a complex multi-agent scenario.

Future work will involve tightening the under-approximation of the segment predicate ATR while addressing redundancy in the computation. We will also aim to make the MILP encoding more efficient. We further wish to more extensively incorporate real-world constraints and perform real-world experiments on a multi-agent system with an event-triggered replanning strategy.

REFERENCES

- [1] L. Lindemann, A. Rodionova, and G. Pappas, “Temporal robustness of stochastic signals,” in *Proceedings of the 25th ACM International Conference on Hybrid Systems: Computation and Control*, 2022, pp. 1–11.
- [2] O. Maler and D. Nickovic, “Monitoring temporal properties of continuous signals,” in *International Symposium on Formal Techniques in Real-Time and Fault-Tolerant Systems*. Springer, 2004, pp. 152–166.
- [3] V. Raman, A. Donzé, M. Maasoumy, R. M. Murray, A. Sangiovanni-Vincentelli, and S. A. Seshia, “Model predictive control with signal temporal logic specifications,” in *53rd IEEE Conference on Decision and Control*. IEEE, 2014, pp. 81–87.
- [4] N. Mehdiipour, C.-I. Vasile, and C. Belta, “Average-based robustness for continuous-time signal temporal logic,” in *2019 IEEE 58th Conference on Decision and Control (CDC)*. IEEE, 2019, pp. 5312–5317.
- [5] M. Vahs, C. Pek, and J. Tumova, “Risk-aware spatio-temporal logic planning in gaussian belief spaces,” in *International Conference on Robotics and Automation*, 2023.
- [6] G. E. Fainekos and G. J. Pappas, “Robustness of temporal logic specifications for continuous-time signals,” *Theoretical Computer Science*, vol. 410, no. 42, pp. 4262–4291, 2009.
- [7] A. Donzé and O. Maler, “Robust satisfaction of temporal logic over real-valued signals,” in *International Conference on Formal Modeling and Analysis of Timed Systems*. Springer, 2010, pp. 92–106.
- [8] Z. Lin and J. S. Baras, “Optimization-based motion planning and runtime monitoring for robotic agent with space and time tolerances,” *IFAC-PapersOnLine*, vol. 53, no. 2, pp. 1874–1879, 2020.
- [9] A. Rodionova, L. Lindemann, M. Morari, and G. J. Pappas, “Time-robust control for stl specifications,” in *2021 60th IEEE Conference on Decision and Control (CDC)*. IEEE, 2021, pp. 572–579.
- [10] A. Rodionova, L. Lindemann, M. Morari, and G. Pappas, “Temporal robustness of temporal logic specifications: Analysis and control design,” *ACM Transactions on Embedded Computing Systems*, vol. 22, no. 1, pp. 1–44, 2022.
- [11] A. Rodionova, L. Lindemann, M. Morari, and G. J. Pappas, “Combined left and right temporal robustness for control under stl specifications,” *IEEE Control Systems Letters*, vol. 7, pp. 619–624, 2022.
- [12] X. Yu, X. Yin, and L. Lindemann, “Efficient stl control synthesis under asynchronous temporal robustness constraints,” *arXiv preprint arXiv:2307.12855*, 2023.
- [13] Y. E. Sahin, P. Nilsson, and N. Ozay, “Synchronous and asynchronous multi-agent coordination with *ctl+* constraints,” in *2017 IEEE 56th Annual Conference on Decision and Control (CDC)*. IEEE, 2017, pp. 335–342.
- [14] ———, “Multirobot coordination with counting temporal logics,” *IEEE Transactions on Robotics*, vol. 36, no. 4, pp. 1189–1206, 2019.
- [15] C.-I. Vasile, D. Aksaray, and C. Belta, “Time window temporal logic,” *Theoretical Computer Science*, vol. 691, pp. 27–54, 2017.
- [16] D. Sun, J. Chen, S. Mitra, and C. Fan, “Multi-agent motion planning from signal temporal logic specifications,” *IEEE Robotics and Automation Letters*, vol. 7, no. 2, pp. 3451–3458, 2022.
- [17] T. Marcucci, M. Petersen, D. von Wrangel, and R. Tedrake, “Motion planning around obstacles with convex optimization,” *arXiv preprint arXiv:2205.04422*, 2022.
- [18] X. Qian, I. Navarro, A. de La Fortelle, and F. Moutarde, “Motion planning for urban autonomous driving using bézier curves and mpc,” in *2016 IEEE 19th international conference on intelligent transportation systems (ITSC)*. Ieee, 2016, pp. 826–833.
- [19] L. Gurobi Optimization, “Gurobi optimizer reference manual,” 2021.